Data Repository Material for "Fault zone characteristics and basin complexity in the southern Salton Trough, California"

DOI:10.1130/G38033.1

Patricia Persaud[1], Yiran Ma[1], Joann M. Stock[1], John A. Hole[2], Gary S. Fuis[3] and Liang Han[2]
[1] *California Institute of Technology, Seismological Laboratory, Pasadena, CA 91125, USA*
[2] *Virginia Polytechnic Institute and State University, Blacksburg, VA 24061, USA*
[3] *U. S. Geological Survey, Menlo Park, CA 94025, USA*

Supplementary Material

The supplementary figures included here show the following in relationship to the main text:

Figure DR1. The seismicity catalog from which the seismicity lineaments (L1-L4) discussed in the text were determined. A short explanation of the significance of L1-L4 and how they were determined is included in the figure caption.

Figure DR2. A-B: Aerial photo showing a NE-trending vegetation lineament in a field near the Wienert Fault supporting our interpretation of NE-trends in seismicity as significant structures.

Figure DR3. A: The 2-D model, which is the same as one shown in Fig. 2 of the manuscript, but is plotted here down to 40-km depth. The green line in Fig. 1 of the manuscript shows the profile location. **B:** The corresponding ray coverage to 40-km depth. **C:** The initial smoothed CVM-H model.

Figure DR4. A-D: The ray coverage at 1-, 3-, 5-, and 7-km depths corresponding to the 3-D model results shown in Fig. 3 of the manuscript. Note, in Fig. 3 the regions with no crossing rays are shaded gray.

Figure DR5. A-D: 3-D model inversion results using only the explosive source data for comparison to the results in Fig. 3 of the manuscript, which includes earthquake data.

The seismic velocity results from this study are being incorporated into the Southern California Earthquake Center Community Velocity Model with support from the Southern California Earthquake Center. SCEC is funded by NSF Cooperative Agreement EAR-1033462 & USGS Cooperative Agreement C12AC20038.

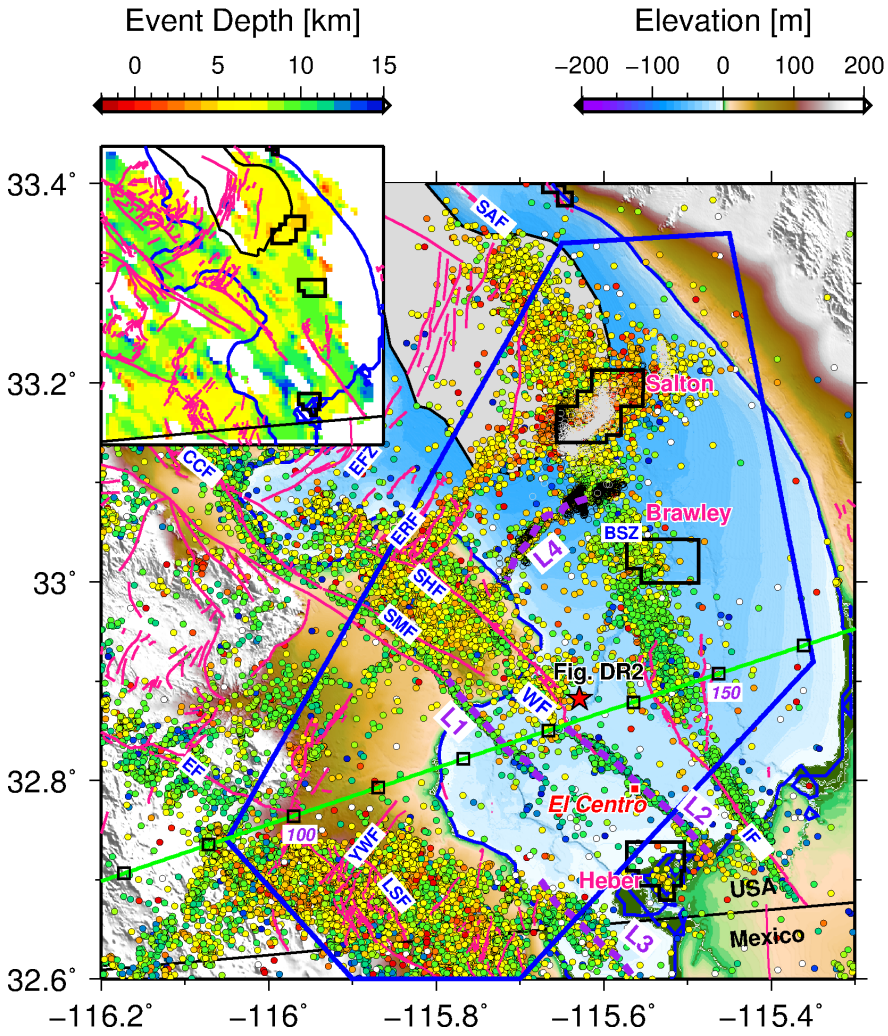

Figure DR1. Color-shaded earthquake depths from the catalog of Hauksson et al. (2012). Inset map shows the average earthquake depth in 0.025° ×0.025° bins. Small black and gray circles in the larger map are relocated earthquakes from the 1981 and 2005 earthquake swarms, respectively, from Lohman and McGuire (2007). Seismicity lineaments (dashed purple lines), L1-L4 are discussed in the main text. The prominent seismicity trends were picked by hand, and are based on the Hauksson et al. (2012) catalog. L1, L2 and L3 also correspond to similarly named seismicity trends of Magistrale (2002) with some notable differences. In Magistrale (2002), L1 extends farther south into the Heber geothermal area than our trend, and merges with the Superstition Mountain fault in the north, and L3 corresponds to the Cerro Prieto seismicity lineament which is mapped farther south than in this study. Magistrale (2002) did not interpret a trend similar to L4 although NE-trending seismicity alignments are noted in their Fig. 2 that coincide with L4, and more subtle NE-trends are present in addition to L4. Our L4 trend aligns with the relocated 1981 swarm (black circles) from Lohman and McGuire (2007) even though we used a different catalog to pick our trend. There are several NE-trends in the seismicity that may be significant structures. We also note a NE-striking vegetation lineament (red star) in a field near the Wienert fault, which is shown in Fig. DR2. This feature may correspond to the New River cross fault described by Sedgwick (1941). Faults (pink lines) are compiled from

Fenby and Gastil (1991), Jennings and Bryant (2010), and Rockwell et al. (2015). Geothermal areas labeled and outlined in black are from the Division of Oil, Gas & Geothermal Resources (http://www.conservation.ca.gov/dog/geothermal/maps). The sea level contour (blue outline), location of our 2D model (green line from Fig. 1 in the main text), and 3D model domain (blue polygon) are shown. BSZ-Brawley Seismic Zone, CCF-Coyote Creek fault, EF-Elsinore fault, EFZ-Extra fault zone, ERF-Elmore Ranch fault, IF-Imperial fault, LSF-Laguna Salada fault, SAF-San Andreas fault, SHF-Superstition Hills fault, SMF-Superstition Mountain fault, WF-Wienert fault, YWF-Yuha Wells fault.

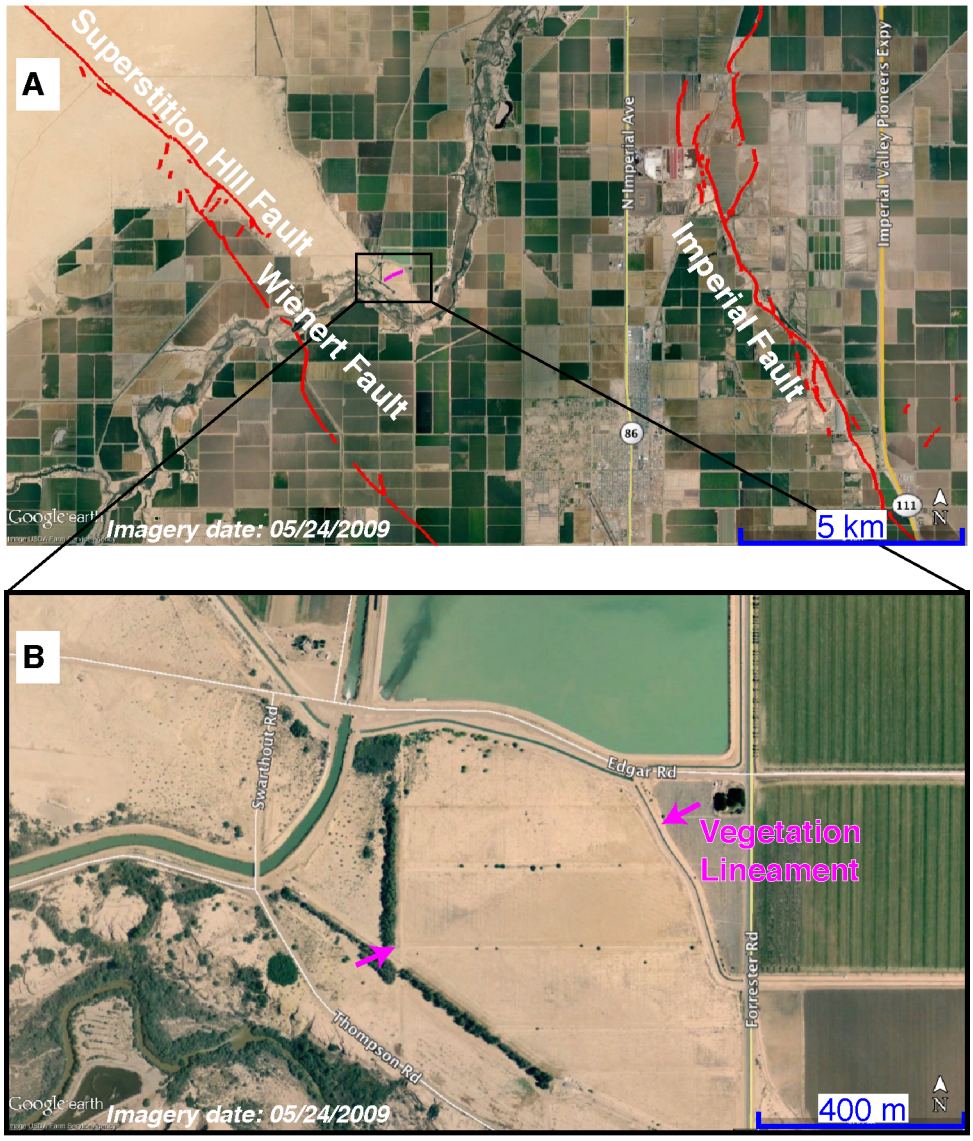

Figure DR2. A: Google Earth imagery from 05/24/2009 showing the location of a NE-trending vegetation lineament (pink line) in a field located east of the Wienert Fault. See the red star in Fig. DR1 for the location in a more zoomed out map. This lineament was also discussed by Sedgwick (1941) as possibly related to the New River cross fault. A closer view of the vegetation lineament is shown in **(B)**.

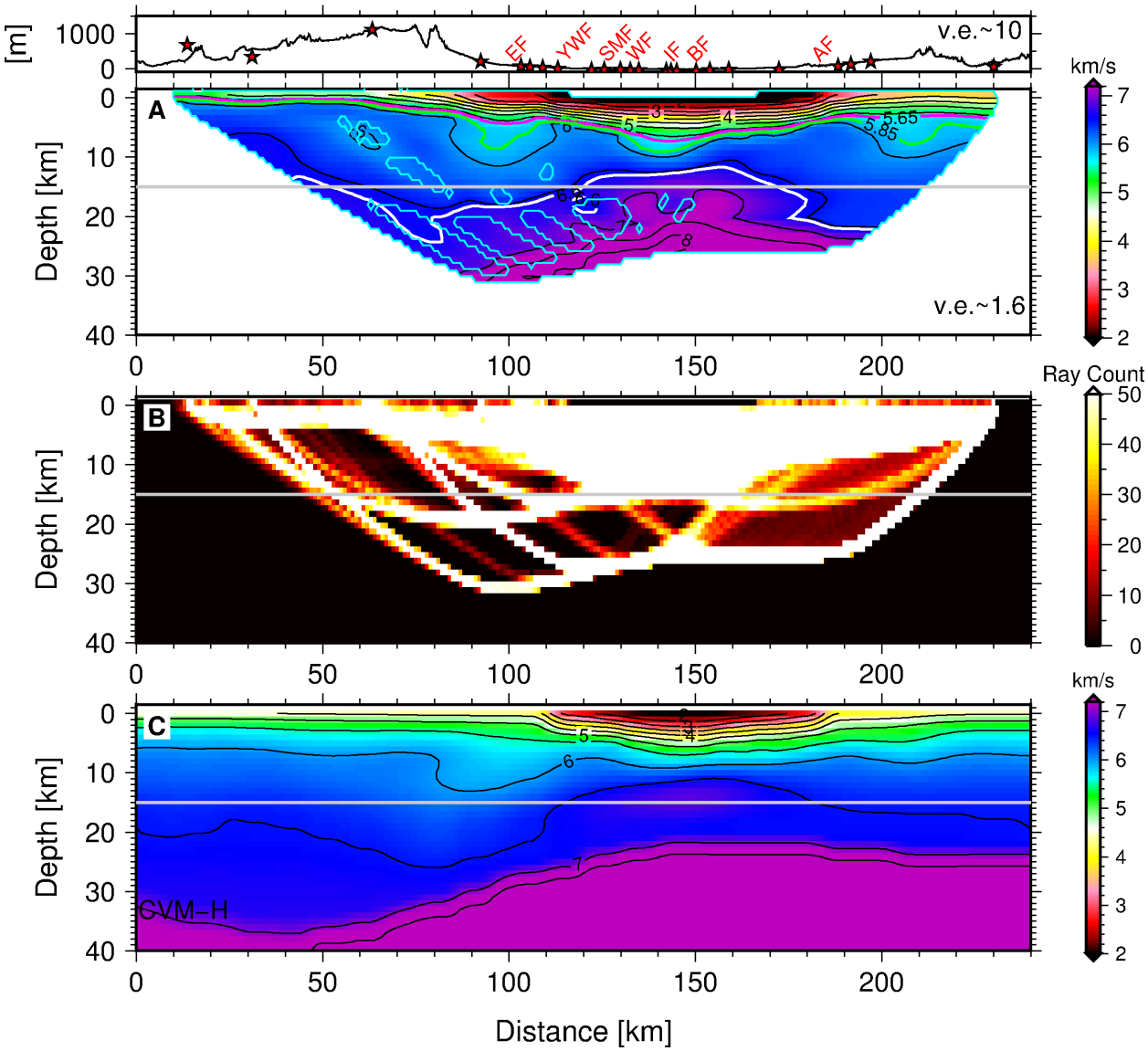

Figure DR3. A: The P-wave velocity structure along the profile (green line) in Fig. 1, with faults projected along strike labeled above the topography in the top panel. The inversion is performed on 1×1 km grid. The cyan lines enclose the region with coverage. Velocity contours at 5.65 km/s (purple), 5.85 km/s (green) and 6.6 km/s (white) are shown**. B:** The number of rays in each grid cell. **C:** The initial 5-km smoothed CVM-H model. We show the results in regions with good ray coverage (above the gray lines in A-C) in Fig. 2 of the manuscript at a different vertical exaggeration. AF-Algodones fault, BF-Brawley Fault, EF-Elsinore fault, IF-Imperial fault, SMF-Superstition Mountain fault, WF-Wienert fault, YWF-Yuha Wells fault.

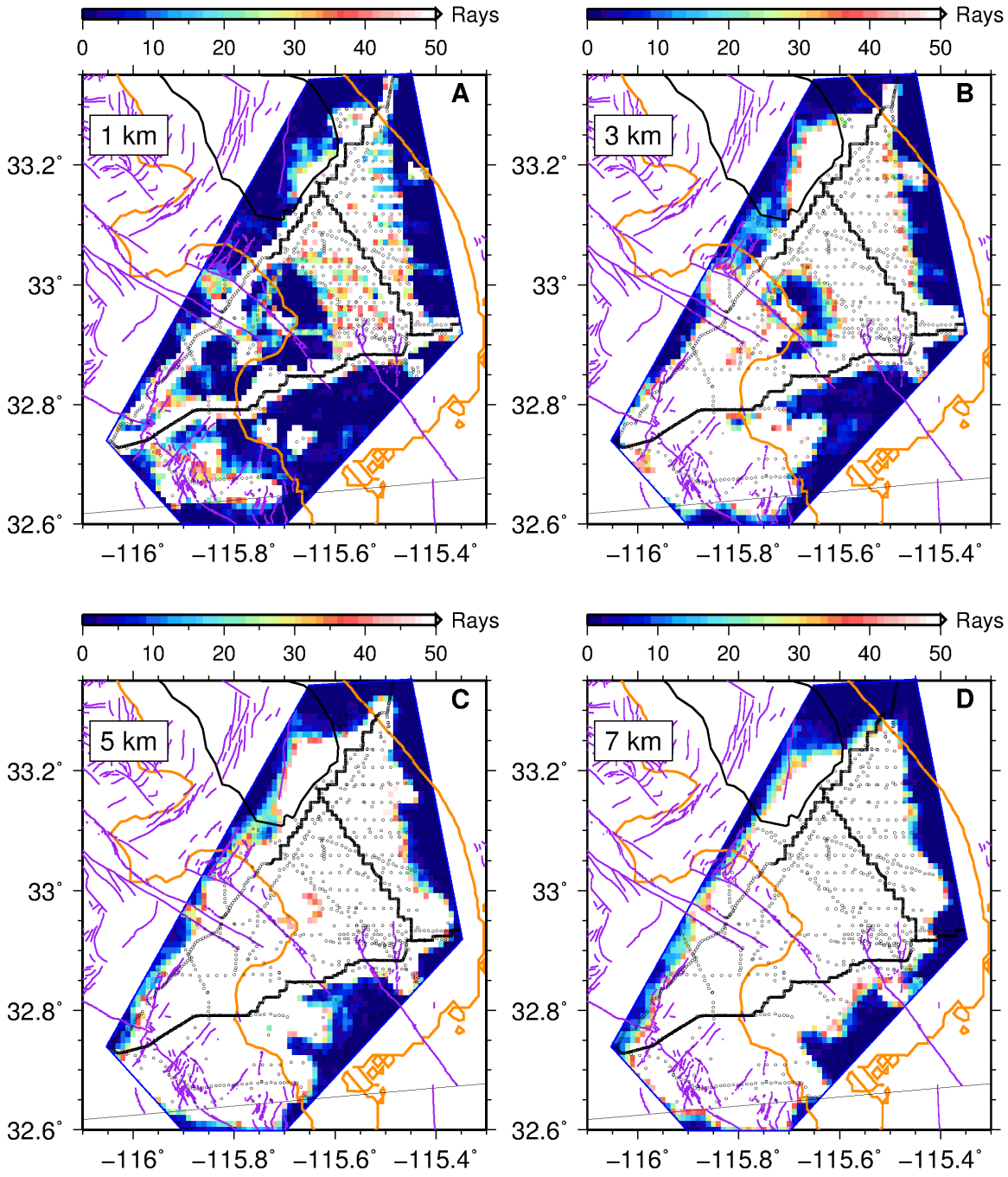

Figure DR4. The number of rays in each 1×1×1 km grid cell of the 3-D model shown in Fig. 3 of the manuscript. Faults (purple lines), receivers (small white circles with black outlines), and the sea level contour (orange line) are shown.

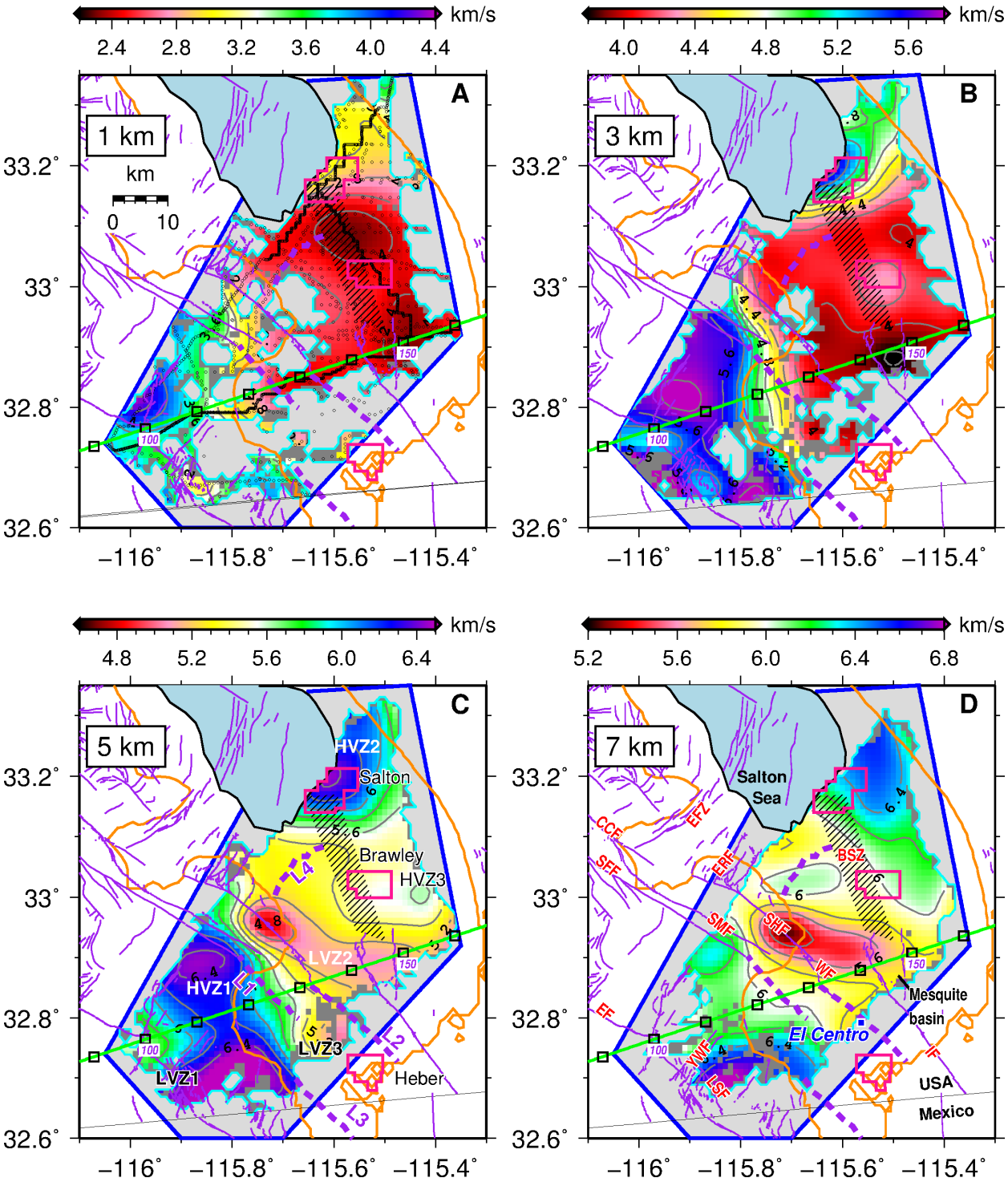

Figure DR5. The 3-D inversion results using explosion data only (SSIP and IV1979). The grids with no ray penetration are shown in gray. Note the different color scales in each panel. Location of the velocity profile shown in Figs. 1 and 2 (green line), receivers (small black circles in A), geothermal areas from Division of Oil, Gas & Geothermal Resources (pink outlines, labels in C; http://www.conservation.ca.gov/dog/geothermal/maps), sea level contour (orange line), regions with ray penetration from shots (cyan lines) and active faults (purple lines, labels in D) are

shown. Hatched area of the BSZ and the seismicity lineaments (dashed purple lines, L1-L4 in C) are based on the seismicity in Fig. DR1. **C:** High-velocity (HVZ1-HVZ3), and low-velocity zones (LVZ1-LVZ3) discussed in the text. BSZ-Brawley Seismic Zone, CCF-Coyote Creek fault, EF-Elsinore fault, EFZ-Extra Fault Zone, ERF- Elmore Ranch fault, IF-Imperial fault, LSF-Laguna Salada fault, SFF-San Felipe fault, SHF-Superstition Hills fault, SMF-Superstition Mountain fault, WF-Wienert fault, YWF-Yuha Wells fault.

REFERENCES CITED

Fenby, S. S., and Gastil, R. G., 1991, Geologic-tectonic map of the Gulf of California and surrounding areas, *in* Dauphin, J. P., and Simoneit, B. R. T., eds., The Gulf and Peninsular Provinces of the Californias, American Association of Petroleum Geologists Memoir 47: Tulsa, Oklahoma, p. 79–83, doi: 10 .1306 /M47542C6.

Hauksson, E., Yang, W., and Shearer, P. M., 2012, Waveform relocated earthquake catalog for Southern California (1981 to June 2011): Bulletin of the Seismological Society of America, v. 102, no. 5, p. 2239-2244, doi: 10 .1785 /0120120010.

Jennings, C. W., and Bryant, W. A., 2010, Fault activity map of California: California Geological Survey Geologic Data Map No. 6, map scale 1:750,000.

Lohman, R. B., and McGuire, J. J., 2007, Earthquake swarms driven by aseismic creep in the Salton Trough, California: Journal of Geophysical Research: Solid Earth, v. 112, no. B4, doi: 10.1029/2006JB004596.

Magistrale, H., 2002, The relation of the southern San Jacinto fault zone to the Imperial and Cerro Prieto faults: Special Paper - Geological Society of America, *in* Barth, A., ed., Contributions to crustal evolution of the southwestern United States: Geological Society of America Special Paper 365, p. 271–278, doi: 10 .1130 /0 -8137 -2365 -5 .271.

Rockwell, T. K., Fletcher, J. M., Teran, O. J., Hernandez, A. P., Mueller, K. J., Salisbury, J. B., Akciz, S. O., and Štěpančíková, P., 2015, Reassessment of the 1892 Laguna Salada Earthquake: Fault Kinematics and Rupture Patterns: Bulletin of the Seismological Society of America, v. 105, p. 2885–2893, doi: 10.1785/0120140274.

Sedgwick, A. E., 1941, Location of major fault zones in the Imperial Valley for Imperial Irrigation District, El Centro, California, Los Angeles, Allan E. Sedgwick, 34 p. (This is a report completed by A. Sedgwick for the Imperial Valley Irrigation District.)